

Ultrafast electric field controlled spin correlations in the Hubbard model

Nagamalleswararao Dasari* and Martin Eckstein†

Department of Physics, University of Erlangen-Nuremberg, 91058 Erlangen, Germany

 (Received 29 March 2019; revised manuscript received 6 September 2019; published 30 September 2019)

Highly intense electric field pulses can move the electronic momentum occupation in correlated metals over large portions of the Brillouin zone, leading to phenomena such as dynamic Bloch oscillations. Using the nonequilibrium fluctuation-exchange approximation for the two-dimensional Hubbard model, we study how such nonthermal electron distributions drive collective spin and charge fluctuations. Suitable pulses can induce a highly anisotropic modification of the occupied momenta, and the corresponding spin dynamics results in a transient change from antiferromagnetic to anisotropic ferromagnetic correlations. To good approximation this behavior is understood in terms of an instantaneous response of the spin correlations to the single-particle properties.

DOI: [10.1103/PhysRevB.100.121114](https://doi.org/10.1103/PhysRevB.100.121114)

Ultrashort and highly intense laser pulses have opened novel pathways to control quantum materials [1,2]. There are many detailed accounts of the ultrafast momentum and energy-resolved electron dynamics, from strongly correlated quasiparticles to band electrons in two-dimensional materials [3–5]. On the other hand, many rich properties of correlated materials arise from the interplay of the electronic structure with charge, spin, and orbital fluctuations, and intriguing pathways for transient light-induced or enhanced orders have been theoretically proposed [6–10]. It is therefore of major interest to understand the interplay between single-particle properties such as electron populations and spectra and the collective two-particle properties on the ultrashort timescale.

An intriguing approach would be to explore this interplay with the help of strong electric fields that can be used to design specific nonequilibrium electron distributions, which then possibly induce a collective response. Nonperturbative electric fields can coherently drive electrons over large portions of the Brillouin zone, enabling Floquet band engineering [11,12] or the observation of Bloch oscillations [13] and Zener tunneling [14] in solids. Because of the rapid electron thermalization, nonthermal electron distributions in metals are not long-lived enough to manipulate long-wavelength fluctuations, in particular close to critical points [15]. However, a clear separation of timescales does not necessarily hold for the collective response at shorter scales, and in the following we demonstrate that even in quickly thermalizing metallic systems field-engineered electron distributions can drive a nontrivial spin response.

We investigate this issue by studying the dynamics of electrons and spin in a moderately correlated metal, using the two-dimensional Hubbard model. Extending on the idea of Refs. [16,17], which proposed to use nonperturbative fields to engineer negative temperature states, we exploit the polarization direction of the pulse to transiently generate highly

asymmetric electron distributions in the Brillouin zone, and investigate the resulting collective (spin) response of the electron system. Our study is focused on the metallic phase. For larger interactions, in the Mott insulator, qualitatively different physics is expected. Both electrons and spins can remain out of equilibrium for a long time [18], and the physics is understood in terms of robust spin moments driven by strong electromagnetic fields directly [19] or through a modification of exchange interactions [20] and photodoping [21].

Model. The Hubbard Hamiltonian is given by

$$H = - \sum_{\langle R,R' \rangle, \sigma} t_{R-R'} c_{R\sigma}^\dagger c_{R'\sigma} + U \sum_R n_{R,\uparrow} n_{R,\downarrow}, \quad (1)$$

where $c_{R\sigma}^\dagger$ creates an electron with spin $\sigma \in \{\uparrow, \downarrow\}$ on site R of a square lattice of size L^2 , U is the repulsive on-site interaction; $t_{R-R'}$ is the nearest-neighbor hopping, corresponding to a dispersion $\epsilon_k(t) = \epsilon_0[\mathbf{k} - \mathbf{A}(t)]$ with $\epsilon_0(\mathbf{k}) = -2t_{\text{hop}}[\cos(k_x a) + \cos(k_y a)]$. We choose units $a = 1$, $e = 1$, $c = 1$ (speed of light), and $\hbar = 1$. The tunneling matrix element $t_{\text{hop}} = 1$ sets the energy scale. We focus on the metallic phase at moderately strong $U \leq 1.5$, before the system would cross over into a regime dominated by antiferromagnetic correlations. The electric field is incorporated in the calculations through the Peierls substitution, with the vector potential $\mathbf{A}(t)$ and $\mathbf{E}(t) = -\frac{1}{c} \partial_t \mathbf{A}(t)$. The field pulses transiently displace the electron distribution over the Brillouin zone, and the polarization of the pulse is used to generate anisotropic distributions (see below). If not stated otherwise, we use a half-cycle pulse of the form $\mathbf{E}(t) = \eta(A_0 \pi / 2t_0) \sin(\pi t / t_0)$ (for $0 < t < t_0$) with polarization $\eta = (1, 0)$. With $t_0 = 4$, the center frequency of the pulse is considerably lower than the bandwidth, so that the excitation protocol rather corresponds to subcycle light-driven dynamics than to off-resonant Floquet engineering. In our units, the amplitude A_0 of the vector potential quantifies the maximal momentum transfer on an electron during the cycle in units of \hbar/a .

Method. The nonequilibrium dynamics of the model is discussed within the Keldysh formalism on the L -shaped

*nagamalleswararao.d@gmail.com

†martin.eckstein@fau.de

time contour \mathcal{C} , suited to study the dynamics of a system which is initially in thermal equilibrium at a given temperature T [22]. We study the dynamics in terms of the contour-ordered electronic Green's functions $G_{R-R'}(t, t') = -i\langle T_{\mathcal{C}} c_{R'}(t) c_R^\dagger(t') \rangle$, and the collective propagator $\chi_{R-R'}^\alpha(t, t') = -i\langle T_{\mathcal{C}} \hat{X}_R^\alpha(t) \hat{X}_{R'}^\alpha(t') \rangle$, where \hat{X}^α can be spin $S_R = \sum_{\sigma\sigma'} c_{R\sigma}^\dagger \tau_{\sigma\sigma'} c_{R\sigma'}$ ($\alpha \equiv s$), or charge $X_R^\alpha = \sum_{\sigma} n_{R\sigma}$ ($\alpha \equiv c$). The spatial Fourier transform is defined as $f_R = \frac{1}{L^2} \sum_q e^{iqR} f_q$. From the contour-ordered functions we obtain time-dependent spectra (see below), the gauge-invariant momentum distribution $\tilde{n}_k(t) = \langle c_{k-A(t)}^\dagger(t) c_{k-A(t)}(t) \rangle = -iG_{k-A(t)}^<(t, t)$, and the spin and charge correlations $C_q^\alpha(t) = \langle \hat{X}_q^\alpha(t) \hat{X}_{-q}^\alpha(t) \rangle = i\chi_q^{\alpha<}(t, t)$.

To study the interplay of electrons and collective fluctuations, we employ the fluctuation-exchange (FLEX) approximation [23], a Φ -derivable (i.e., energy and number-conserving) approximation designed to treat the interaction of electrons with charge, spin, pairing, or orbital fluctuation channels. The formulation of the diagrammatic approach [24] is identical on the Matsubara and on the Keldysh time contour. The approximation for the collective propagators is given by the random-phase approximation (RPA) series

$$\chi_q^\alpha = (1 - U_\alpha \Pi_q)^{-1} * \Pi_q. \quad (2)$$

Here $*$ denotes a convolution in contour time [22], the interaction is $U_c = -U_s = U$ for charge and spin, respectively, and $\Pi_R(t, t') = -iG_R(t, t')G_{-R}(t', t)$ is the bare susceptibility, which is identical for charge and spin in the paramagnetic phase. The electron self-energy is given by the second-order diagram, supplemented by the contributions from the fluctuation self-energy $\Sigma_R^\alpha(t, t') = iU^2 G_R^\alpha(t, t') F_R^\alpha(t, t')$, $F_R^{s/c}(t, t') = [\chi_R^{s/c}(t, t') \pm \frac{1}{2} \chi_R^{s/c}(t, t') \mp \frac{1}{2} \Pi_R(t, t')]$ beyond second order. To study the metallic phase in the repulsive Hubbard model at half filling, where magnetic correlations are dominant, we include only the magnetic fluctuation channel into the self-energy. The numerical simulations are performed on a finite grid of L^2 momenta ($L = 28$ for the results below, which is sufficient to obtain converged results for the short-range correlations under investigation). The numerical implementation is based on the libCNTR nonequilibrium Green's functions library [25].

Results—Single-particle properties. In Figs. 1(a)–1(e) we exemplarily show the momentum occupation $\tilde{n}_k(t)$ for a moderately correlated system ($U = 1.5$). Without interaction U , the pulse would simply shift the electrons by the momentum transfer $\Delta k = \int dt E \equiv A_0$ [$A_0 = (\pi, 0)$ in Fig. 1]. In the interacting case we observe a similar shift if the pulse is not too long, up to a broadening of the distribution by electron-electron scattering. Subsequently, electrons relax back to the band minimum and finally thermalize at elevated temperature, due to the electron-electron scattering U . The kinetic energy e_{kin} is roughly zero after the pulse, because the distribution is symmetrically centered around $k = (\pi, 0)$. While $e_{kin} = 0$ would correspond to infinite temperature, during the relaxation the interaction energy is increased and e_{kin} is decreased, such that the final temperature T_* is of the order of the bandwidth. The thermalization can be confirmed also from the local dynamic response functions (which thermalize at a faster rate than the momentum

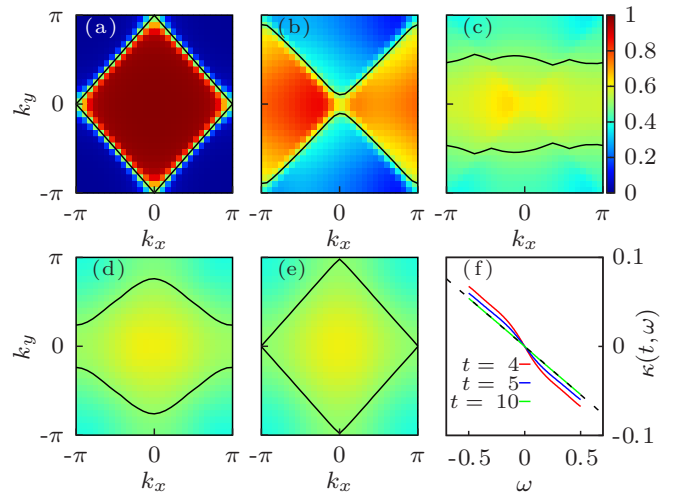


FIG. 1. Momentum distribution $\tilde{n}_k(t)$ at given times t , for the evolution driven by a half-cycle pulse with momentum transfer $\int dt E = A_0 = (\pi, 0)$, and pulse duration $t_0 = 4$, at $U = 1.5$. The distribution is plotted for $t = 0$ [before the pulse, (a)], $t = 4$ [directly after the pulse, (b)], and $t = 9.4, 14.6, 30.0$ [during the relaxation towards the hot-electron state, (c)–(e)]. The solid lines show the surface defined by the occupation $\tilde{n}_k = 0.5$. (f) Logarithmic ratio $\kappa(t, \omega) = \ln[G^<(\omega, t)/G^>(\omega, t)]$, which tends to $\kappa(t, \omega) = -\beta_* \omega$ ($\beta_* = 0.11$, dashed line) in a thermal state with temperature $T_* = 1/\beta_*$.

distribution [26]). Figure 1(f) shows the logarithmic ratio $\kappa(t, \omega) = \ln[G^<(\omega, t)/G^>(\omega, t)]$ for the local Green's function G . [Time-dependent spectra are obtained from the partial Fourier transform $G^{><}(t, \omega) = \pm \text{Im} \int ds G^{><}(t, t-s) e^{i\omega s}$.] The linear relation $\kappa(\omega) = -\omega/T_*$, which is reached for long times, proves that the fluctuation-dissipation theorem is satisfied, such that local single-particle quantities can be considered in thermal equilibrium.

To characterize the dynamics it is interesting to look at the “Fermi surface” defined by $\tilde{n}_k = 0.5$, although for a general nonequilibrium state, this surface neither corresponds to a maximum of the quasiparticle scattering time, nor to a discontinuity in \tilde{n}_k . During the time evolution the surface $\tilde{n}_k = 0.5$ changes from a closed to an open, quasi-one-dimensional topology. Because collective excitations and their instabilities strongly depend on occupied states, this already suggests that the relaxation can have a strong effect on the two-particle correlations.

Before discussing the two-particle physics, we briefly comment on the half-cycle pulse. While $\int dt E = 0$ for a conventional electromagnetic pulse, the half-cycle pulse with $\int dt E \neq 0$ allows us to study in a simple manner both the coherent dynamics during the application of a strong field and the relaxation dynamics in the absence of a field, which can both be accessed in different experimental settings. Furthermore, an asymmetric pulse with $\int dt E = 0$, consisting of an intense first half cycle followed by a longer and weaker second half, would lead to a similar evolution of the single-particle occupations as in Fig. 1. This is verified in the Supplemental Material for different asymmetric pulse shapes [27]. Such asymmetric pulses have been proposed to engineer

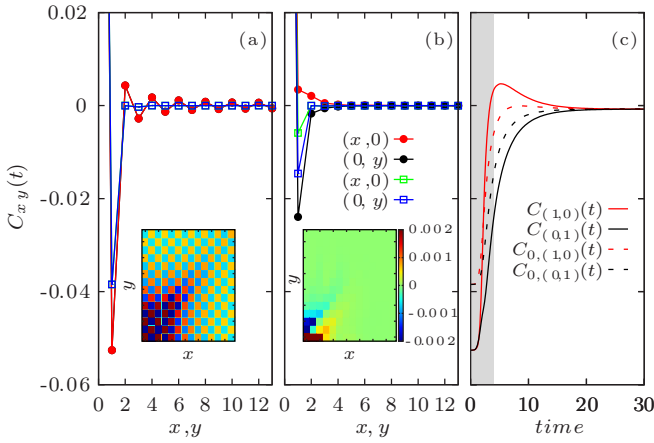


FIG. 2. Spin correlation function $C_R^{(s)}(t)$ along the x and y directions for the same parameters as Fig. 1, at time $t = 0$ (a) and $t = 4 = t_0$ (b). At $t = 0$, the system is still isotropic, $x \equiv y$. Open symbols show the correlations obtained from the bare susceptibility, $C_{0,R}(t)$. The inset shows $C_R^{(s)}(t)$ in false color. (c) Time evolution of the nearest-neighbor correlations $C_{(1,0)}$ and $C_{(0,1)}$ in x and y directions, obtained from the full (solid lines) and bare (dashed lines) spin correlation function. The shaded area indicates the duration of the pulse.

distributions [17], and can lead to a population inversion negative temperature state if the pulse is polarized along the (11) direction.

Results—Spin correlations. Figure 2 shows the real-space spin correlation function $C_R^{(s)}(t) = \langle S_R^z(t) S_0^z(t) \rangle$ for the same set of parameters as Fig. 1. The correlations evolve from short-range antiferromagnetism in the initial state to a strongly thermally suppressed antiferromagnetism in the final state. During the evolution, however, we observe an entirely different pattern, with ferromagnetic correlations along the x direction [see Fig. 2(c) for the nearest-neighbor correlations along the x and y axes] and mixed ferromagnetic/antiferromagnetic correlations along y . In part, a modification of short-range spin correlations is already expected for noninteracting quasiparticles, due to the Pauli principle, as observed after quenches to the noninteracting Hamiltonian [28]. Importantly, one can see that the correlations obtained from the bare susceptibility, $C_{0,R}(t) = i\Pi_R^<(t, t)$, which reflect the statistical correlations of independent electrons, remain antiferromagnetic in all directions throughout the evolution. The reversal of the spin correlations thus happens as a consequence of the collective response.

In general, the change of the electronic occupation modifies the effective action for the collective modes, and thus inflicts a time-dependent force to drive their dynamics. The numerical results show that at least some part of the spin correlations respond faster than the electron thermalization. It is thus interesting to test a scenario which is precisely opposite to the conventional adiabatic separation between fast electrons and slow spin, and in which the spin correlations instead follow the electron dynamics in a quasi-instantaneous manner. As we show below, the numerical results indeed support the latter scenario, as one can rather accurately reconstruct the spin correlations $C_q^{(s)}(t)$ from a nonequilibrium steady state

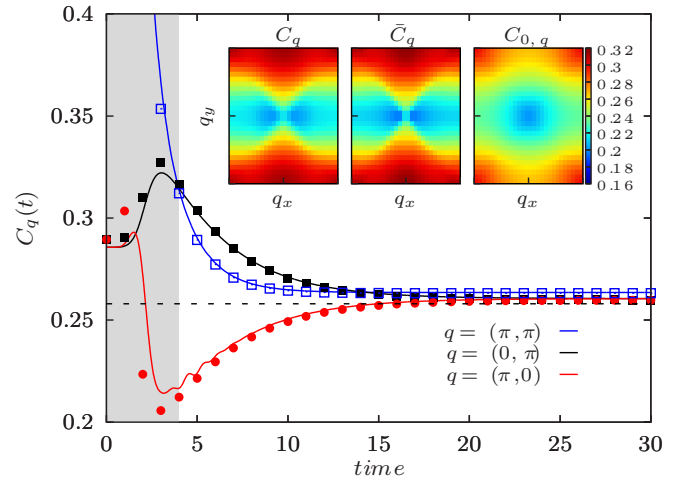


FIG. 3. (a) Correlation $C_q^{(s)}(t)$ (lines) and effective steady state $\bar{C}_q^{(s)}(t)$ (dots with the same color) for three momenta, and the same parameters as Fig. 1. The shaded area indicates the duration of the pulse. The inset shows $C_q^{(s)}$, $\bar{C}_q^{(s)}$, and $C_{0,q}$ in the full Brillouin zone at time $t = 4$. The dashed line indicates the featureless high-temperature state.

that is determined by the electron distribution $\bar{n}_k(t)$ at the same time t .

We start from $\Pi_q(t, t')$, which determines the correlation function of the collective modes through the RPA equation (2). Because the system is weakly interacting, a first-order approximation $\bar{\Pi}_q(\omega; t)$ for $\Pi_q(t, \omega)$ is obtained from the bare response of independent electrons in a nonequilibrium steady state with momentum occupations $\bar{n}_k = \bar{n}_k(t)$. Here and in the following, barred quantities such as \bar{n} and $\bar{\Pi}$ correspond to the nonequilibrium steady state, which depends on time only parametrically. $\bar{\Pi}_q(\omega; t)$ is just given by the Lindhard expression $\bar{\Pi}_q^<(\omega; t) = \frac{1}{L^2} \sum_k \bar{n}_k(t) [1 - \bar{n}_{k-q}(t)] \delta(\epsilon_k - \epsilon_{k-q} - \omega) = \bar{\Pi}_q^>(-\omega; t)$. One can then evaluate Eq. (2) in the 2×2 Keldysh matrix representation, using $\bar{\Pi}_q(\omega)$ as an input to obtain a nonequilibrium steady-state result $\bar{\chi}_q(\omega; t)$, and thus the steady-state correlations $\bar{C}_q(t) = \frac{1}{2\pi i} \int d\omega \bar{\chi}_q^<(\omega; t)$. Figure 3 (inset) shows that the qualitative structure of $C_q^{(s)}(t)$ in the transient state is reproduced by the effective steady state $\bar{C}_q^{(s)}(t)$. Again we emphasize that both $\bar{C}_q^{(s)}(t)$ and $C_q^{(s)}(t)$ differ from the bare response $C_{0,q}(t) = i\Pi_q^<(t, t)$, which retains its maximum at the antiferromagnetic point $\mathbf{q} = (\pi, \pi)$, while the collective response develops a maximum at $(0, \pi)$. The lines in the main panel of Fig. 3 show that the comparison is quantitatively accurate for the characteristic momenta $\mathbf{q} = (\pi, \pi)$, $(\pi, 0)$, $(0, \pi)$ for all times, which confirms the quasi-instantaneous response of the spin to the electrons. In accordance with the real-space picture [Fig. 2(c)], the antiferromagnetic correlations at $\mathbf{q} = (\pi, \pi)$ get strongly suppressed ($C_q^{(s)} \approx 0.25$ corresponds to a featureless high-temperature state), while correlations along the q_x and q_y axes are enhanced and reversed, respectively.

The fast response of the spin can be further explained by looking at the spectral function $-\frac{1}{\pi} \text{Im} \chi_q^R(t, \omega)$ of the collective modes (Fig. 4). The latter is obtained by partial Fourier transform $\chi_q^R(t, \omega) = \int_0^{s_{\max}} ds e^{i\omega s} \chi_q^R(t, t-s)$, where

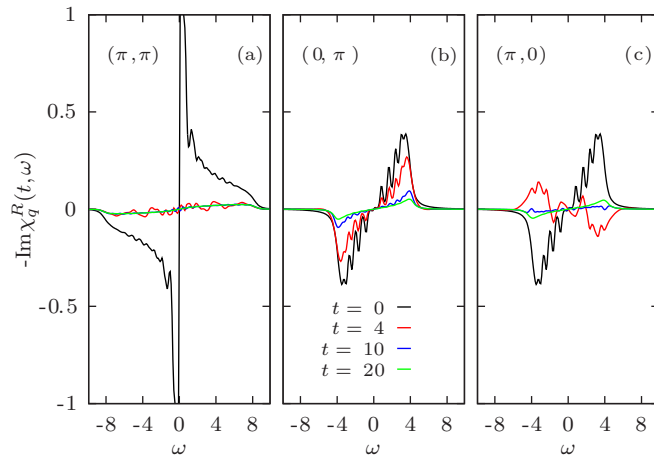


FIG. 4. Spectra of spin correlations for the same excitation as in Fig. 1, at $\mathbf{q} = (\pi, \pi)$ (a), $\mathbf{q} = (0, \pi)$ (b), and $\mathbf{q} = (\pi, 0)$ (c), for initial time $t = 0$, directly after the pulse $t = 4$, and during the relaxation. Note that at $\mathbf{q} = (\pi, 0)$ negative spectral weight is formed as a consequence of the electronic population inversion in this direction.

the superscript R denotes the retarded component, and s_{\max} is set by the simulated time. An *exact* interpretation of the RPA equation (2) is that a collective field with response function χ^R is driven by a stochastic force due to electronic quantum and thermal fluctuations with autocorrelations proportional to $i\Pi_{\mathbf{q}}^<(t, t')$ [29,30]. Hence, if both the response time set by χ^R and the autocorrelation time set by the noise is of the order of the bandwidth, the spin correlations can follow the single-electron state on the inverse hopping time. In the initial state at $t = 0$, slow modes at $\mathbf{q} = (\pi, \pi)$ exist because of the vicinity of the antiferromagnetic instability [narrow peak close to $\omega = 0$ in Fig. 4(a)]. These features are, however, quickly suppressed with time, leading to response with a spectral width of the order of the bandwidth, i.e., few inverse hoppings in the time domain.

The spin response on the tunneling timescale indicates that the antiadiabatic behavior of the short-range spin correlations will become more accurate towards weaker interactions, because electron thermalization slows down like U^{-2} . (The absolute value of the collective response of course decreases in this limit). We have performed simulations for a wide range of interactions, different pulse amplitudes $A_0 \equiv (A_0, 0)$ and pulse durations t_0 , and found that the reversal of spin correlations is indeed a rather robust feature. Figure 5 shows the duration t_* of the time interval where reversal $C_{(\pi, \pi)}^{(s)}(t) < C_{(0, \pi)}^{(s)}(t)$ is observed, which increases with decreasing U [Fig. 5(a)] in agreement with the argument above. Even a full cycle $A_0 = 2\pi$ can reverse the correlations [Fig. 5(b)]. Finally, simulations confirm that also the charge response of the system is rapid, but without significant features in the repulsive Hubbard model at half-filling.

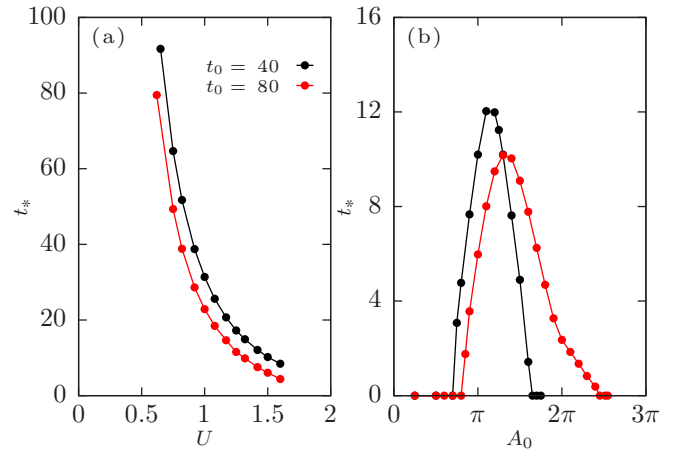


FIG. 5. The duration of reversal of spin correlations for different values of U and pulse durations t_0 (a), and for different pulse amplitudes A_0 at $U = 1.5$ (b).

In conclusion, we have shown that nonthermal electrons can quasi-instantaneously drive a nontrivial spin response in a correlated metal. This opens the intriguing possibility to observe *collective* electron dynamics driven by ultrastrong terahertz fields on the subcycle timescale. While we have focused on spin correlations, which should be dominant in prototypical Slater-type antiferromagnets such as NaOsO_3 [31], analogous effects should be observed for charge correlations in materials which display charge-density wave transitions, such as TiS_2 and TiSe_2 [32]. The laser pulses needed to engineer nonthermal electron distributions should transfer a momentum comparable to the Brillouin zone size \hbar/a (a is the lattice spacing) in one cycle, and a cycle duration should be shorter than the thermalization time τ . This gives field amplitudes of order $E_0 = \hbar/e a \tau \sim 10^7\text{--}10^8$ V/m for $a \sim 10^{-9}$ m and $\tau = 10\text{--}100$ fs. Such fields have been used to drive subcycle dynamics on the single-particle level [13] without permanent material damage. The corresponding magnetic fields E/c are of order one Tesla and thus give a Zeeman splitting which is still much smaller than the relevant electronic energy scales U and hopping. Though challenging, the collective physics might be accessible with time-resolved electron-energy-loss spectroscopy (for the charge correlations), time-resolved x-ray spectroscopy from free-electron-laser sources, or using noise correlations in time-resolved photoemission, which should be accessible through state-of-the-art momentum microscopes [33].

Acknowledgments. We acknowledge discussions with J. Li, A. Lichtenstein, E. Stepanov, Ch. Stahl, and Ph. Werner. This work was supported by the ERC Starting Grant No. 716648. The calculations have been done at the RRZE of the University Erlangen-Nuremberg.

[1] D. N. Basov, R. D. Averitt, and D. Hsieh, *Nat. Mater.* **16**, 1077 (2017).

[2] C. Giannetti, M. Capone, D. Fausti, M. Fabrizio, F. Parmigiani, and D. Mihailovic, *Adv. Phys.* **65**, 58 (2016).

[3] I. Gierz, F. Calegari, S. Aeschlimann, M. Chávez Cervantes, C. Cacho, R. T. Chapman, E. Springate, S. Link, U. Starke, C. R. Ast, and A. Cavalleri, *Phys. Rev. Lett.* **115**, 086803 (2015).

- [4] R. Bertoni, C. W. Nicholson, L. Waldecker, H. Hübener, C. Monney, U. De Giovannini, M. Puppini, M. Hoesch, E. Springate, R. T. Chapman, C. Cacho, M. Wolf, A. Rubio, and R. Ernstorfer, *Phys. Rev. Lett.* **117**, 277201 (2016).
- [5] J. D. Rameau, S. Freutel, A. F. Kemper, M. A. Sentef, J. K. Freericks, I. Avigo, M. Ligges, L. Rettig, Y. Yoshida, H. Eisaki, J. Schneeloch, R. D. Zhong, Z. J. Xu, G. D. Gu, P. D. Johnson, and U. Bovensiepen, *Nat. Commun.* **7**, 13761 (2016).
- [6] M. A. Sentef, A. F. Kemper, A. Georges, and C. Kollath, *Phys. Rev. B* **93**, 144506 (2016).
- [7] M. Knap, M. Babadi, G. Refael, I. Martin, and E. Demler, *Phys. Rev. B* **94**, 214504 (2016).
- [8] Y. Murakami, N. Tsuji, M. Eckstein, and P. Werner, *Phys. Rev. B* **96**, 045125 (2017).
- [9] A. Nava, C. Giannetti, A. Georges, E. Tosatti, and M. Fabrizio, *Nat. Phys.* **14**, 154 (2017).
- [10] J. Li, H. U. R. Strand, P. Werner, and M. Eckstein, *Nat. Commun.* **9**, 4581 (2018).
- [11] Y. H. Wang, H. Steinberg, P. Jarillo-Herrero, and N. Gedik, *Science* **342**, 453 (2013).
- [12] J. W. McIver, B. Schulte, F.-U. Stein, T. Matsuyama, G. Jotzu, G. Meier, and A. Cavalleri, [arXiv:1811.03522](https://arxiv.org/abs/1811.03522).
- [13] O. Schubert, M. Hohenleutner, F. Langer, B. Urbanek, C. Lange, U. Huttner, D. Golde, T. Meier, M. Kira, S. W. Koch, and R. Huber, *Nat. Photonics* **8**, 119 (2014).
- [14] T. Higuchi, C. Heide, K. Ullmann, H. B. Weber, and P. Hommelhoff, *Nature (London)* **550**, 224 (2017).
- [15] Y. Lemonik and A. Mitra, *Phys. Rev. B* **96**, 104506 (2017); **98**, 214514 (2018).
- [16] N. Tsuji, T. Oka, P. Werner, and H. Aoki, *Phys. Rev. Lett.* **106**, 236401 (2011).
- [17] N. Tsuji, T. Oka, H. Aoki, and P. Werner, *Phys. Rev. B* **85**, 155124 (2012).
- [18] N. Walldorf, D. M. Kennes, J. Paaske, and A. J. Millis, *Phys. Rev. B* **100**, 121110(R) (2019).
- [19] T. Kampfath, A. Sell, G. Klatt, A. Pashkin, S. Mährlein, T. Dekorsy, M. Wolf, M. Fiebig, A. Leitenstorfer, and R. Huber, *Nat. Photonics* **5**, 31 (2010).
- [20] F. Görg, M. Messer, K. Sandholzer, G. Jotzu, R. Desbuquois, and T. Esslinger, *Nature (London)* **553**, 481 (2018).
- [21] J. H. Mentink and M. Eckstein, *Phys. Rev. Lett.* **113**, 057201 (2014).
- [22] H. Aoki, N. Tsuji, M. Eckstein, M. Kollar, T. Oka, and P. Werner, *Rev. Mod. Phys.* **86**, 779 (2014).
- [23] N. E. Bickers, D. J. Scalapino, and S. R. White, *Phys. Rev. Lett.* **62**, 961 (1989).
- [24] N. Bickers and D. Scalapino, *Ann. Phys. (NY)* **193**, 206 (1989).
- [25] M. Schueler, D. Golež, H. U. R. Strand, N. Bittner, Ph. Werner, and M. Eckstein (unpublished).
- [26] M. Moeckel and S. Kehrein, *Phys. Rev. Lett.* **100**, 175702 (2008).
- [27] See Supplemental Material at <http://link.aps.org/supplemental/10.1103/PhysRevB.100.121114> for more details about the drive along (1,1) direction, double occupancy and spin correlations for asymmetric pulse shapes.
- [28] I. G. White, R. G. Hulet, and K. R. A. Hazzard, *Phys. Rev. A* **100**, 033612 (2019).
- [29] A. Kamenev, [arXiv:cond-mat/0412296](https://arxiv.org/abs/cond-mat/0412296).
- [30] In order to explain this notion of a noise-driven spin dynamics, it is convenient to resort to the Hubbard-Stratonovich field $\phi_q(t)$ with propagator $F_q(t, t') = [U_s^{-1} - \Pi_q]^{-1} = U_s \chi_q^{(s)} U_s + U_s$, whose fluctuations $F_q^< = U_s^2 \chi_q^<$ are directly related to the spin. Following Langreth rules, the equation for the lesser component of the field is $F_q^< = F_q^R * \Pi_q^< * F_q^A$. This equation is equivalently represented by $iF_q^<(t, t') = \langle \phi_{-q}(t') \phi_q(t) \rangle_\xi$, where ϕ_q responds to a time-dependent force $\xi_q(t)$ according to the equation $\phi_q(t) = \int_{-\infty}^t dt' F_q^R(t, t') \xi_q(t')$, and the average $\langle \dots \rangle_\xi$ is taken over a stochastic force with autocorrelation $\langle \xi_{-q}(t') \xi_q(t) \rangle_\xi = i\Pi_q^<(t, t')$.
- [31] Y. G. Shi, Y. F. Guo, S. Yu, M. Arai, A. A. Belik, A. Sato, K. Yamaura, E. Takayama-Muromachi, H. F. Tian, H. X. Yang, J. Q. Li, T. Varga, J. F. Mitchell, and S. Okamoto, *Phys. Rev. B* **80**, 161104(R) (2009).
- [32] S. Hellmann, T. Rohwer, M. Källäne, K. Hanff, C. Sohrt, A. Stange, A. Carr, M. M. Murnane, H. C. Kapteyn, L. Kipp, M. Bauer, and K. Rossnagel, *Nat. Commun.* **3**, 1069 (2012).
- [33] C. Stahl and M. Eckstein, *Phys. Rev. B* **99**, 241111(R) (2019).